

# Matter-Wave Imaging of Quantum Density Fluctuations in Ultracold Bosons in an Optical Lattice

Scott N. Sanders,<sup>1</sup> Florian Mintert,<sup>1,2</sup> and Andreas Buchleitner<sup>1</sup>

<sup>1</sup>*Albert-Ludwigs-Universität Freiburg, Hermann-Herder-Str. 3, 79104 Freiburg, Germany*

<sup>2</sup>*Freiburg Institute for Advanced Studies, Albertstr. 19, 79104 Freiburg, Germany*

(Dated: February 7, 2017)

We study the influence of quantum density fluctuations in ultracold atoms in an optical lattice on the scattering of matter waves. Such fluctuations are characteristic of the superfluid phase and vanish due to increased interactions in the Mott insulating phase. We employ an analytical treatment of the scattering and demonstrate that the fluctuations lead to incoherent processes, which we propose to observe via decoherence of the fringes in a Mach-Zender interferometer. In this way we extract the purely coherent part of the scattering. Further, we show that the quantum density fluctuations can also be observed directly in the differential angular scattering cross section for an atomic beam scattered from the atoms in a lattice. Here we find an explicit dependence of the scale of the inelastic scattering on the quantum density fluctuations.

## I. INTRODUCTION

The atoms in a weakly interacting Bose Einstein condensate flow as a superfluid over the crystalline potential landscape formed by a periodic pattern of light intensity. Individual atoms in this system can be spatially delocalized over the breadth of the optical lattice, and, as a consequence, fluctuations in the number of atoms at individual lattice sites occur even at zero temperature. As the repulsion between the atoms grows, they are driven into a Mott insulating phase, in which they maximally isolate themselves and localize to a single lattice site [1–3]. This rigid crystal, which reflects the behavior of tightly bound electrons hopping in a solid, develops as the atoms spontaneously lock to fixed, integer occupation of each lattice site, and the fluctuations vanish.

Our objective is to study the influence of these quantum mechanical fluctuations on the scattering of matter waves, and to illustrate the susceptibility of the scattering to this purely quantum mechanical effect, as well as the consequent impact of the transition from non-interacting single particle physics to strongly interacting, many body physics. Ultracold atoms in an optical lattice are an ideal context in which to examine this behavior because they allow controlled investigation of the transition between single and many body physics, due to the experimental tunability of the physical parameters of the crystal: the tunneling rate between lattice sites, the interaction strength between atoms in the lattice and the geometry of the lattice [3–5].

It has been proposed that light scattering from atoms in an optical lattice, situated within an optical cavity, will be sensitive to the on-site number statistics [6]. Moreover, recent experiments with high resolution optical systems have demonstrated images resolving features on the scale of a single lattice site both for atoms collected from a magneto-optic trap [7, 8] and for atoms in a Bose-Einstein condensate [5, 9]. Due to the interactions of the atoms with the light, however, only the parity of the number of atoms at each site can be directly observed; nonetheless, the fluctuations in the parity display a dependence on the many body phase of the atoms in the lattice.

The scattering cross section of ultracold atoms in an optical lattice seen by a matter wave probe is sensitive to the quantum many body phase in the lattice [10]. We seek to understand the specific influence of the exotic properties of these materials on the images produced by matter waves and to employ this knowledge to make non-destructive measurements. Here, we study the effect of the purely quantum mechanical density fluctuations at individual lattice sites and show that these zero-temperature fluctuations can be directly probed using a matter wave.

Fluctuations in the density distribution seen by an imaging matter wave are expected to produce a dephasing effect and lead to incoherent scattering. By examining the overlap of the matter wave scattered from the atoms in an optical lattice with a coherent reference beam, in an interferometric configuration, we will be able to explicitly see the decohering effect of quantum density fluctuations on the interference pattern, and to determine the size of the density fluctuations. Subsequently, we will show that this incoherent scattering can even be observed in the angular differential scattering cross section, and that the scale of the fluctuations can be obtained directly by examining the inelastic part of the scattering in an appropriate regime of probe energy and lattice depth.

The matter wave probe is a free particle with mass  $m$ , initial wave vector  $\mathbf{k}_0$  and Hamiltonian  $H_P = \hat{\mathbf{p}}^2/2m$ , which does not interact with the lattice light. The scattering target is well modeled by the Bose Hubbard Hamiltonian, describing  $N$  atoms confined to the lowest band of a lattice with  $N_L$  sites,

$$\hat{H}_{\text{BH}} = -J \sum_{\langle \mathbf{R}, \mathbf{R}' \rangle} \hat{a}_{\mathbf{R}}^\dagger \hat{a}_{\mathbf{R}'} + \frac{1}{2} U \sum_{\mathbf{R}} \hat{n}_{\mathbf{R}} (\hat{n}_{\mathbf{R}} - 1). \quad (1)$$

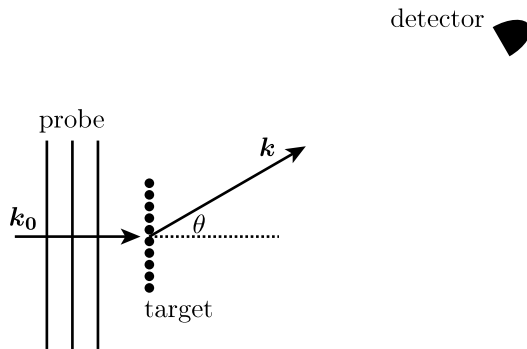


FIG. 1. Scattering configuration in which the probe matter wave is incident from the left upon a one-dimensional lattice. A detector in the far-field measures the flux of probe atoms scattered in the direction  $\theta$ .

For a sufficiently large lattice, in which the effects of the edges of the lattice are negligible, we may impose periodic boundary conditions on both the atoms in the lattice and the transverse dimensions of the probe. We may freely choose our coordinate system so that the  $z$ -axis is aligned with  $\mathbf{k}_0$ . The initial probe wave function is then given by

$$\langle \mathbf{r} | \mathbf{k}_0 \rangle = \frac{e^{ik_0 z}}{\sqrt{2\pi L^2}}, \quad (2)$$

where  $k_0$  is the magnitude of  $\mathbf{k}_0$ , and  $L$  is the length of the lattice in the transverse dimensions.

As we wish our probe to weakly interact with the atoms in the lattice, and to avoid interband excitations, we will insist on low energy probes, for which s-wave scattering from the atoms in the target is dominant, and we may treat the interaction between the probe and the atoms in the lattice as a pseudopotential with scattering length,  $a_s$ . The scattering interaction is then given by [11],

$$\hat{V} = \sum_j V_0 \delta(\hat{\mathbf{r}} - \hat{\mathbf{r}}_j), \quad (3)$$

where the operators  $\hat{\mathbf{r}}$  and  $\hat{\mathbf{r}}_j$  give the positions of the probe and the  $j^{\text{th}}$  lattice atom, respectively, and  $V_0 = 2\pi\hbar^2 a_s/m$ . The full Hamiltonian for the scattering interaction is  $\hat{H} = \hat{H}_P + \hat{H}_{BH} + \hat{V}$ .

## II. INTERFERENCE MEASUREMENT OF DENSITY FLUCTUATIONS

A standard scattering configuration, as depicted in Fig. 1, in which the angular differential scattering cross section is measured, does not specifically distinguish coherent from incoherent scattering. The possibility that disturbances are created in the target, such as long wavelength phonons, exists despite the presence of evidence in the scattering pattern for coherent scattering processes, such as Bragg peaks. Insofar as these disturbances do not completely localize the probe, interference of its wave function scattered from separated points in the lattice can persist.

The situation is starkly different if the probe is coherently split into two beams before scattering, so that there is a reference beam that does not interact with the target. Interference between the atom scattered from the target and the reference beam will then take place only if the probe scatters without disturbing the target at all. We will confirm the incoherent effect of the quantum density fluctuations in the lattice on the scattered probe specifically by employing the Mach-Zender configuration shown in Fig. 2 [12, 13].

In this arrangement, the upper arm scatters from the sample of cold atoms in the optical lattice and then interferes downstream with the lower arm. The interference pattern that forms there will be due solely to the coherent part of the scattering, in which the state of the atoms in the lattice is undisturbed [14, 15]. In practice, the narrow angular acceptance of the region of overlap, where the detector is placed, also restricts detection to the essentially forward scattered atoms [16, 17]. The forward scattered beam may, however, acquire a phase shift and be attenuated due to incoherent scattering. Both of these quantities, the phase shift and attenuation, can be directly observed in the interference pattern that forms. Here, we are particularly interested in analyzing the attenuation, as this indicates the amount of incoherent scattering, and, as we demonstrate below, depends on the zero-temperature density fluctuations.

In order to determine this phase shift and attenuation, we consider the S-matrix for the multi-particle system, which connects the initial many body state of the probe and target with the asymptotic output state,  $|\psi\rangle$ , long after

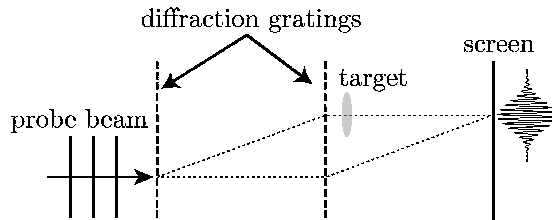


FIG. 2. Schematic of the Mach-Zender interferometer arrangement in which the probe beam is incident on a diffraction grating from the left. The 0<sup>th</sup> and 1<sup>st</sup> order diffracted beams form the lower and upper arms of the interferometer, respectively. The second diffraction grating causes the arms of the interferometer to overlap downstream at the position of the screen. A target is placed in the path of the upper arm only, so that only the coherent scattering will interfere with the lower, reference arm.

the scattering interaction has ceased [18],

$$|\psi\rangle = \hat{S} |\mathbf{k}_0, n_0\rangle. \quad (4)$$

The initial wave vector of the probe is labeled  $\mathbf{k}_0$ , and  $|n_0\rangle$  is the many body ground state of the  $N$  atoms in the lattice. The operator  $\hat{S}$  can be expanded generically in terms of the total energy  $E$  of the  $N + 1$  atoms, the transition operator  $\hat{T}$  and the Hamiltonian  $\hat{H}_0$ , which excludes interactions [19],

$$\hat{S} = 1 - 2\pi i \delta(E - \hat{H}_0) \hat{T}. \quad (5)$$

For the system we are discussing, the non-interacting Hamiltonian is given by  $\hat{H}_0 = \hat{H}_P + \hat{H}_{BH}$ , and the transition operator is given by [20],

$$\hat{T} = \hat{V} + \lim_{\epsilon \rightarrow 0} \hat{V} \frac{1}{E_0 + E_{n_0} - \hat{H}_P - \hat{H}_{BH} + i\epsilon} \hat{T}. \quad (6)$$

The operator

$$\hat{G}_0^{(N+1)} = \left( E_0 + E_{n_0} - \hat{H}_P - \hat{H}_{BH} + i\epsilon \right)^{-1} \quad (7)$$

is the free Green's operator for the many body system.  $E_0$  is the initial energy of the probe, and  $E_{n_0}$  is the energy of the target ground state. The state of the  $N + 1$  particle system that results from the scattering, in terms of these operators, is

$$|\psi\rangle = |\mathbf{k}_0, n_0\rangle - 2\pi i \delta(E - \hat{H}_0) \hat{T} |\mathbf{k}_0, n_0\rangle. \quad (8)$$

The first term is the unscattered initial state. In the Mach-Zender configuration, this term is coherent with the reference arm. The second term involves both coherent and incoherent contributions. We can facilitate extraction of the coherent contribution by expanding in terms of eigenstates of the non-interacting probe and target. This is accomplished by interposing a complete set of probe and target states between the delta function and the operator  $\hat{T}$ . We may then exclude contributions to the scattering that create disturbances in the target or deflect the probe out of the forward direction. Choosing the direction of  $\mathbf{k}_0$  to align with the  $z$ -axis of our coordinate system and recalling that the probe is subject to periodic boundary conditions in the transverse dimensions, the expansion yields

$$|\psi\rangle = |\mathbf{k}_0, n_0\rangle - 2\pi i \int dk_z \sum_{k_x, k_y} \sum_n \delta(E - \hat{H}_0) |k_x, k_y, k_z, n\rangle \langle k_x, k_y, k_z, n | \hat{T} |\mathbf{k}_0, n_0\rangle. \quad (9)$$

Any scattering interaction which changes the state of the target, such that  $n \neq n_0$ , would cause the probe to decohere completely, so that we may exclude all such terms from the sum over target states. As we mentioned above, the small angular acceptance of the detector requires that we also exclude deflection of the probe in the  $x - y$  plane. The remaining integral over  $k_z$  may then be performed immediately. The coherent part of the system after scattering is given by

$$|\psi_{coh}\rangle = \left( 1 - i \frac{2\pi m}{\hbar^2 k_0} \langle k_0, n_0 | \hat{T} | k_0, n_0 \rangle \right) |k_0, n_0\rangle, \quad (10)$$

where, for simplicity, we write  $|k_0\rangle$  as short hand for  $|0, 0, k_0\rangle$ , in which the components of the probe wave vector in the  $x$  and  $y$  directions are zero. Eq. (10) does not yet incorporate the specific details of our target, and is written here in general for any scattering matrix  $\hat{T}$  and initial target state  $|n_0\rangle$ . The diagonal  $T$ -matrix element of the initial state is the crucial quantity that determines both the phase shift and the contrast of the interference fringes. We may identify the complex amplitude of the coherent wave, given in Eq. (10), with the expansion of an exponential when the strength of the interaction  $V_0$  between the probe and the atoms in the target is weak [21]. The coherent amplitude can then be separated into a part which corresponds to a phase shift,  $\phi = -\frac{2\pi m}{\hbar^2 k_0} \text{Re}(\langle \hat{T} \rangle)$ , and an attenuation,  $\xi = -\frac{2\pi m}{\hbar^2 k_0} \text{Im}(\langle \hat{T} \rangle)$ , where both expectation values are taken in the initial state,  $|k_0, n_0\rangle$ . The coherent part of the scattering in terms of these quantities is

$$|\psi_{\text{coh}}\rangle = (1 + i\phi - \xi) |k_0, n_0\rangle \approx e^{i\phi - \xi} |k_0, n_0\rangle. \quad (11)$$

We may read off from this expression that the interference pattern that forms will be shifted by  $\phi$  and the fringes will have a contrast  $e^{-\xi}$  [14, 15].

It is appropriate to consider the case of weak interactions as we seek to probe the target without disturbing its state. The values of  $\phi$  and  $\xi$  will then be dominated by the lowest-order terms in a Born expansion of the operator  $\hat{T}$ , defined by Eq. (6). To first order in  $V_0$ , the transition operator coincides with the interaction potential ( $\hat{T} \approx \hat{V}$ ), so that the  $T$ -matrix element becomes  $\langle k_0, n_0 | \hat{V} | k_0, n_0 \rangle$ . This quantity is purely real, and gives us the leading order phase shift of the interference pattern. To first order in  $V_0$ , however, there is no attenuation, and the scattering is purely coherent. Loss of contrast in this system arises in the second order correction,  $\hat{T} \approx \hat{V} + \hat{V} \hat{G}_0^{(N+1)} \hat{V}$ . The second order contribution to the  $T$ -matrix element,  $\langle k_0, n_0 | \hat{V} \hat{G}_0^{(N+1)} \hat{V} | k_0, n_0 \rangle$ , is in general complex-valued. The real part of it will contribute a small correction to the phase shift  $\phi$ , and the imaginary part gives the leading order approximation of  $\xi$ .

In order to facilitate our intuition of the relationship between  $\phi$  and  $\xi$  and the moments of the density distribution of the atoms in the lattice, we will express the interaction potential in second quantized form, in which it is given by

$$\hat{V} = V_0 \hat{n}(\hat{\mathbf{r}}_0). \quad (12)$$

Here  $\hat{n}(\mathbf{r}) = \hat{\psi}^\dagger(\mathbf{r})\hat{\psi}(\mathbf{r})$  is the density of the target at the position  $\mathbf{r}$ . Inasmuch as the interaction potential depends linearly on  $\hat{n}(\mathbf{r})$ , an expansion of the  $T$ -matrix in a Born series, in orders of  $V_0$ , will contain terms that depend upon a corresponding moment of the density distribution. For this reason,  $\phi$ , whose leading contribution is linear in  $V_0$ , will depend solely on the average density of the target. Likewise,  $\xi$ , which is second order in  $V_0$ , will depend on the second moment of the density distribution of atoms in the target, and therefore on the fluctuations.

Let us now explicitly evaluate the phase shift and decoherence of the probe. As we explained above, the phase shift requires that we evaluate the diagonal  $T$ -matrix element in the first Born approximation, which yields

$$\langle k_0, n_0 | \hat{T} | k_0, n_0 \rangle \approx \frac{V_0}{2\pi L^2} \int d^3 r \langle n_0 | \hat{n}(\mathbf{r}) | n_0 \rangle. \quad (13)$$

We find that, for any  $|n_0\rangle$ , to first order in the interaction strength, in which only single scattering events are included in the expansion of the  $T$ -matrix, the coherently scattered wave depends only on the average density of the many body target,

$$|\psi_{\text{coh}}\rangle = \exp\left(-i\frac{2\pi a_s \rho}{k_0}\right) |k_0, n_0\rangle. \quad (14)$$

The approximation of the phase shift given by Eq. (14) is proportional to the column density,  $\rho = N/L^2$ , of the atoms in the target. This result is not restricted to the case of cold atoms in an optical lattice, and is known to determine, for example, the phase shift due to scattering from a thermal gas [15, 16, 22, 23].

By allowing terms that are second order in  $V_0$ , we enable scattering channels in which the probe scatters from two different atoms within the target, and thereby becomes sensitive to density fluctuations. The coherent part of the scattered wave to second order is,

$$|\psi_{\text{coh}}\rangle = \left(1 - \frac{2\pi i m}{\hbar^2 k_0} \left(\langle k_0, n_0 | \hat{V} | k_0, n_0 \rangle + \langle k_0, n_0 | \hat{V} \hat{G}_0^{(N+1)} \hat{V} | k_0, n_0 \rangle\right)\right) |k_0, n_0\rangle. \quad (15)$$

As we argued above, the imaginary part of the second order term gives us the exponent in the fringe contrast to leading order, so that we must evaluate

$$\xi = -\frac{2\pi m}{\hbar^2 k_0} \text{Im} \left[ \langle k_0, n_0 | \hat{V} \hat{G}_0^{(N+1)} \hat{V} | k_0, n_0 \rangle \right]. \quad (16)$$

We will isolate the dependence of  $\xi$  on the density fluctuations and determine the extent of their impact on the suppression of the fringe contrast. This can be accomplished analytically in the regime in which the energy of the probe,  $E_0 = \hbar^2 k_0^2 / (2m)$ , is large compared to the bandwidth of the optical lattice, but not sufficiently large to excite atoms out of the lowest band, so that we continue to have single band dynamics. The optical lattice potential along each spatial direction is  $V_L(x) = V_L \sin^2(x)$ , where the depth of the lattice is conveniently specified in units of the photon recoil energy  $E_r = \hbar^2 k_L^2 / (2m_T)$ .  $k_L$  is the laser wave number, and  $m_T$  is the mass of an atom in the target. For a typical lattice depth of  $V_L = 15E_r$ , the width of the lowest band, determined by the energy difference between the center and the edge of the first Brillouin zone, is found from the exact solution for the optical lattice eigenvalue equation to be  $0.03E_r$ . Likewise, the gap between the first and second bands, determined by the energy difference between these bands at the edge of the first Brillouin zone, is  $6.28E_r$ . It is, therefore, readily possible to employ a probe with energy much larger than the lowest band's width, which is nonetheless insufficient to bridge the band gap. In this situation, we may neglect the loss of energy by the probe. The second order term in the expansion of the diagonal  $T$ -matrix element that appears in Eq. (10) is

$$\langle k_0, n_0 | \hat{V} \hat{G}_0^{(N+1)} \hat{V} | k_0, n_0 \rangle = \frac{V_0^2}{2\pi L^2} \int d^3r d^3r' e^{i\mathbf{k}_0 \cdot (\mathbf{r}' - \mathbf{r})} \langle n_0 | \hat{n}(\mathbf{r}) \hat{G}_0^{(N+1)}(\mathbf{r}, \mathbf{r}'; E_0 + E_{n_0}) \hat{n}(\mathbf{r}') | n_0 \rangle. \quad (17)$$

The matrix element in this expression has a clear physical interpretation. The probe wave function is scattered first at  $\mathbf{r}'$ , with a strength proportional to the density of atoms in the target at this location. The scattered probe then evolves freely according to the Green's function from  $\mathbf{r}'$  to  $\mathbf{r}$ , where a second scattering event takes place. As we are computing the coherently scattered projectile wave function, we only include the contribution to this process which leaves the target untouched, in the state  $|n_0\rangle$ . We then integrate over all such two-point scattering paths.

Although the target must be left untouched, there may be transient excitations between the two scattering events. Formally, this can be seen by inserting a complete set of target states,  $\sum_n |n\rangle \langle n|$ , into the transition matrix element in Eq. (17). Note that the eigenstates of the target,  $|n\rangle$ , are also eigenstates of the many body Green's function,

$$\sum_n \hat{G}_0^{(N+1)}(\mathbf{r}, \mathbf{r}'; E_0 + E_{n_0}) |n\rangle \langle n| = \sum_n \langle \mathbf{r} | \frac{1}{E_0 + (E_{n_0} - E_n) - \hat{H}_P + i\epsilon} | \mathbf{r}' \rangle |n\rangle \langle n|. \quad (18)$$

The coefficients in this expansion are the usual, single particle free Green's functions at the shifted energy  $\epsilon_n = E_0 + (E_{n_0} - E_n)$ ,

$$\hat{G}_0(\mathbf{r}, \mathbf{r}'; \epsilon_n) = \langle \mathbf{r} | \frac{1}{\epsilon_n - \hat{H}_P + i\epsilon} | \mathbf{r}' \rangle. \quad (19)$$

Physically, each term corresponds to an intermediate inelastic scattering channel, in which the projectile has transferred energy  $E_n - E_{n_0}$  to the target. The largest possible energy transfer due to scattering a single atom in the target within the lowest band is the bandwidth. As we are considering the situation in which the initial probe energy is large compared to the bandwidth of the lowest band, the transient shift in its energy will be comparatively small, so that  $\epsilon_n \approx E_0$ . The single particle Green's function that appears in the expansion in Eq. (18) is, therefore, approximately independent of the sum over target states. Inserting this expansion into the second-order correction to the  $T$ -matrix element given in Eq. (17) yields

$$\langle k_0, n_0 | \hat{V} \hat{G}_0^{(N+1)} \hat{V} | k_0, n_0 \rangle \approx \frac{V_0^2}{2\pi L^2} \int d^3r d^3r' e^{i\mathbf{k}_0 \cdot (\mathbf{r}' - \mathbf{r})} G_0(\mathbf{r}, \mathbf{r}'; E_0) \langle n_0 | \hat{n}(\mathbf{r}) \hat{n}(\mathbf{r}') | n_0 \rangle. \quad (20)$$

In arriving at this expression, we have made use of the fact that the projectile loses very little energy as it passes through the target, and that interactions with individual atoms in the target are predominantly s-wave scattering, due to the slow relative velocities. The amplitude for each individual double scattering sequence appropriately depends on the density-density correlator between the two scattering points.

As we seek the relationship between the on-site particle number fluctuations in the lattice and the decay of the contrast of the interference fringes, we must express the density-density correlator in Eq. (20) in terms of the on-site field operators. The field operator for the atoms in the target can be expanded in terms of the Wannier function for the lowest band of the lattice,  $w(\mathbf{r})$ , as

$$\hat{\psi}(\mathbf{r}) = \sum_{j=1}^{N_L} \hat{a}_j w(\mathbf{r} - \mathbf{R}_j), \quad (21)$$

where the operator  $\hat{a}_j$  annihilates a particle at the  $j^{\text{th}}$  lattice site. The density  $\hat{n}(\mathbf{r})$ , in terms of this expansion, is then given by

$$\hat{n}(\mathbf{r}) = \sum_{j,k=1}^{N_L} \hat{a}_j^\dagger \hat{a}_k w^*(\mathbf{r} - \mathbf{R}_j) w(\mathbf{r} - \mathbf{R}_k). \quad (22)$$

For the lattice depths that we are considering,  $V_L \sim 15E_r$ , we may employ the tight-binding approximation and neglect the off-diagonal terms due to the small overlap between Wannier functions centered on different lattice sites. The relationship between the density at a position  $\mathbf{r}$  and the density at a site,  $j$ , is then approximately

$$\hat{n}(\mathbf{r}) \approx \sum_{j=1}^{N_L} \hat{n}_j |w(\mathbf{r} - \mathbf{R}_j)|^2. \quad (23)$$

Substituting this into the density-density correlator will allow us to explicitly extract the dependence on the fluctuations,

$$\langle n_0 | \hat{n}(\mathbf{r}) \hat{n}(\mathbf{r}') | n_0 \rangle \approx \sum_{j,k=1}^{N_L} \langle \hat{n}_j \hat{n}_k \rangle |w(\mathbf{r} - \mathbf{R}_j)|^2 |w(\mathbf{r}' - \mathbf{R}_k)|^2. \quad (24)$$

When the number of atoms  $N$  in the target is much larger than 1, a condensate of  $N$  atoms in the ground state of the lattice is well approximated by a coherent state with an average of  $N$  atoms. In the weakly interacting case, therefore, the target ground state is appropriately described as a product of coherent states at each lattice site with an average of  $\bar{n}$  atoms per site [3, p. 906]. In the strongly interacting case, the target is a product of Fock states with  $\bar{n}$  atoms per site. In either case, we may simplify the cross correlators between different lattice sites,  $\langle \hat{n}_j \hat{n}_k \rangle = \langle \hat{n}_j \rangle \langle \hat{n}_k \rangle$  ( $j \neq k$ ), so that these correlators are independent of the many body phase. For a uniform lattice, the average density does not vary from site to site, so that  $\langle n_j \rangle = \bar{n} = N/N_L$ . The diagonal terms in the sum yield a dependence on the second moment of the on-site number distribution, which is also independent of the particular index,  $j$ . The second moment can be re-expressed in terms of the on-site fluctuations,  $\sigma$ , as  $\sigma^2 = \langle \hat{n}_j^2 \rangle - \bar{n}^2$ . The contribution of the square of the average density may be combined with the off-diagonal terms to give a sum over all pairs of sites, leaving

$$\langle n_0 | \hat{n}(\mathbf{r}) \hat{n}(\mathbf{r}') | n_0 \rangle \approx \sigma^2 \sum_{j=1}^{N_L} |w(\mathbf{r} - \mathbf{R}_j)|^2 |w(\mathbf{r}' - \mathbf{R}_j)|^2 + \bar{n}^2 \sum_{j,k=1}^{N_L} |w(\mathbf{r} - \mathbf{R}_j)|^2 |w(\mathbf{r}' - \mathbf{R}_k)|^2. \quad (25)$$

The second term in the density-density correlator, proportional only to the average density, will not vary as the interaction strength is increased across the transition between the superfluid and Mott insulating phases; however, the first term, proportional to the density fluctuations, will vanish as the interaction strength between the atoms in the lattice increases, becoming zero in the Mott insulator. The appearance of fluctuations in the diagonal  $T$ -matrix element will lead to an additional loss of contrast in the interference fringes. Inserting this expression for the density-density correlator into the expression for the second order contribution to the  $T$ -matrix element given in Eq. (20) yields

$$\langle \mathbf{k}_0, n_0 | \hat{V} \hat{G}_0^{(N+1)} \hat{V} | \mathbf{k}_0, n_0 \rangle = \frac{V_0^2 \sigma^2 N_L}{2\pi L^2} F^{(2)}(\mathbf{k}_0) + A, \quad (26)$$

where  $A$  refers to the contribution of the term proportional to  $\bar{n}^2$ . This quantity is independent of the interaction strength as the average density of atoms per lattice site is fixed for any  $U/J$  and will therefore not contribute to the variation of the interference fringe contrast. The function  $F^{(2)}(\mathbf{k}_0)$  gives the amplitude for all possible two-point scattering events,

$$F^{(2)}(\mathbf{k}_0) = \int d^3 r d^3 r' e^{i\mathbf{k}_0 \cdot (\mathbf{r}' - \mathbf{r})} |w(\mathbf{r})|^2 G_0(\mathbf{r}, \mathbf{r}'; E_0) |w(\mathbf{r}')|^2. \quad (27)$$

The imaginary part of  $F^{(2)}(\mathbf{k}_0)$  is calculated in Appendix A for the concrete situation in which the lattice is one-dimensional and oriented perpendicular to the incident probe beam (see Fig. 1). It is then given by

$$\text{Im} \left( F^{(2)}(\mathbf{k}_0) \right) = -\frac{mk_L}{\hbar^2 2^{3/2} \sqrt{\pi}} s^{1/4} \text{Erf} \left( \frac{k_0/k_L}{\sqrt{2} s^{1/4}} \right), \quad (28)$$

where  $s = V_L/E_r$  is the depth of the lattice in units of the photon recoil energy. Using this, we can explicitly write down the factor that modifies the contrast of the interference fringes due to the quantum mechanical density fluctuations in the lattice,

$$C \propto \exp\left(-\frac{\rho a_s^2}{k_0/k_L} \frac{\sigma^2}{\bar{n}} \frac{s^{1/4}}{\sqrt{\pi} 2^{3/2}} \operatorname{Erf}\left(\frac{k_0/k_L}{\sqrt{2} s^{1/4}}\right)\right). \quad (29)$$

Here we note that the functional dependence of the contrast on the wave number of the probe and the depth of the lattice is in terms of the dimensionless quantity  $K = (k_0/k_L)/(\sqrt{2} s^{1/4})$ . Employing  $K$ , the factor giving the reduction of the contrast due to the fluctuations in the lattice takes the form

$$C \propto \exp\left(-\frac{\rho a_s^2}{4\sqrt{\pi}} \frac{\sigma^2}{\bar{n}} \frac{1}{K} \operatorname{Erf}(K)\right). \quad (30)$$

For a typical lattice depth,  $s = 15$ , and for the range of probe wave numbers which avoid interband excitations at this lattice depth,  $k_0/k_L \leq \sqrt{6.28}$ , the variation of the exponent with  $K$  is minor, and the function,  $K^{-1} \operatorname{Erf}(K)$  is of order 1. The remaining dependence of the contrast is such that it decays exponentially with increasing fluctuations in the on-site atom number and with increasing column density of the sample.

The attenuation of contrast given in Eq. (30) can be directly obtained from experimental measurement of the interference fringes as the ratio of the contrast of the fringes at arbitrary values of the parameter  $U/J$  to the contrast deep in the Mott insulator regime, where  $\sigma^2 \rightarrow 0$ . Although it is common to alter the interaction strength  $U/J$  by adjusting the depth of the lattice, here we consider adjusting  $U/J$  by manipulating the scattering length of the lattice atom collisions through a Feshbach resonance, so that we retain a constant lattice depth, and  $K$  remains constant.

We have shown that the quantum mechanical density fluctuations at individual lattice sites have a decohering effect on a matter wave passing through a Mach-Zender interferometer, and that the contrast in the interference fringes is exponentially suppressed by increasing fluctuations. It was necessary to employ an interferometric arrangement to explicitly extract the coherent component of the scattering, and in this way, we have definitively verified the enhancement of incoherent scattering due to these density fluctuations. In the following section, we will exploit these results to identify the influence of the density fluctuations on the scattering cross section and demonstrate the conditions under which the fluctuations are directly observable therein.

### III. DENSITY FLUCTUATIONS AND INELASTIC SCATTERING

We begin our analysis of the differential scattering cross section with a general result for scattering from a many body system in the first Born approximation. The target is initially in the ground state,  $|n_0\rangle$ . The cross section is then given by [10, 22]

$$\frac{d\sigma}{d\Omega} = a_s^2 \sum_n \sqrt{1 - \frac{E_n - E_{n_0}}{\hbar^2 k_o^2 / (2m)}} \left| \langle n | \sum_{j=1}^N e^{i\boldsymbol{\kappa} \cdot \hat{\mathbf{r}}_j} | n_0 \rangle \right|^2, \quad (31)$$

where  $\boldsymbol{\kappa} = \mathbf{k}_0 - \mathbf{k}$  is the difference between the incident probe wave vector  $\mathbf{k}_0$  and the outgoing probe wave vector  $\mathbf{k}$ . The magnitude of  $\mathbf{k}$  is potentially reduced from the incident probe wave number, due to a transfer of energy from the probe to the lattice, and is determined by  $\hbar^2 k^2 / (2m) = \hbar^2 k_o^2 / (2m) + (E_{n_0} - E_n)$ . The outgoing probe wave vector points in the direction  $\theta$  of the detector (see Fig. 1).

Bragg peaks, which correspond to a coherent sum of waves scattered from individual atoms in the lattice, appear in the elastic scattering cross section [10]. Additionally, we showed in Sec. II that increased density fluctuations correspond to increased incoherent scattering of the probe. This suggests that the on-site density fluctuations will influence the scattering cross section through inelastic channels, in which the probe delivers energy to the atoms in the lattice. This intuition motivates us to examine the cross section under the same energetic conditions as in our analysis of the interference pattern in Sec. II, described immediately following Eq. (16). There, the contribution of single band inelastic channels was emphasized by choosing an initial probe energy sufficient to allow excitation to all of the modes of the lowest band of the lattice, but which did not exceed the splitting between the lowest band and the first excited band.

The transition amplitude between the ground state,  $n_0$ , and an excited state,  $n$ , due to a momentum boost, which is given by the matrix element in the expression for the cross section in Eq. (31), is non-zero in the first Born approximation only for final target states in which at most a single atom in the target is displaced out of the ground state of the lattice. The energy of the final target modes that we must consider,  $E_n$ , differ, therefore, from  $E_0$  by the

energy of a single particle excitation. Thus, the conditions are viable to enforce the condition  $E_n - E_{n_0} \ll \hbar^2 k_o^2 / (2m)$  for all accessible final target states. At such high probe energies, the factor under the square root in Eq. (31), which weights the contribution of the scattering into the final target mode,  $n$ , is nearly uniform and approximately unity. This factor appears also in  $\kappa$ ; however, in the high-energy approximation, we take  $\kappa$  to be independent of the energy transfer. This is equivalent to the so-called static approximation [22]. With these simplifications, the cross section becomes

$$\frac{d\sigma}{d\Omega} = a_s^2 \langle n_0 | \sum_{j=1}^N e^{-i\kappa \cdot \hat{\mathbf{r}}_j} \left( \sum_n |n\rangle \langle n| \right) \sum_{k=1}^N e^{i\kappa \cdot \hat{\mathbf{r}}_k} |n_0\rangle. \quad (32)$$

In the subspace of the lowest band of the lattice, the sum over projections onto individual target modes,  $n$ , is an identity and can be removed. The cross section can then be expressed in terms of the density-density correlator, given in Eq. (25), by rewriting it in second quantized notation. This is accomplished via the identification of  $\sum_{k=1}^N e^{i\kappa \cdot \hat{\mathbf{r}}_k}$  with  $\int d^3r e^{i\kappa \cdot \mathbf{r}} \hat{n}(\mathbf{r})$ , which leads to the expression for the cross section,

$$\frac{d\sigma}{d\Omega} = a_s^2 \int d^3r d^3r' e^{-i\kappa \cdot (\mathbf{r} - \mathbf{r}')} \langle n_0 | \hat{n}(\mathbf{r}) \hat{n}(\mathbf{r}') | n_0 \rangle. \quad (33)$$

We may expand the density  $\hat{n}(\mathbf{r})$  according to Eq. (23), in terms of on-site densities and the Wannier function of the lowest band. When the number of lattice sites is sufficiently large that the effect of the edges may be neglected, the cross section separates into two factors. One of which is a smooth background determined by the shape of the Wannier function, which reflects the depth of the lattice. The other depends only on the distribution of atoms in the lattice. Thus for  $N_L \gg 1$ , we find

$$\frac{1}{a_s^2} \frac{d\sigma}{d\Omega} \approx \left( \sum_{j=1}^{N_L} \langle \hat{n}_j^2 \rangle + \sum_{j \neq k} \langle \hat{n}_j \hat{n}_k \rangle e^{i\kappa \cdot (\mathbf{R}_k - \mathbf{R}_j)} \right) \left| \int d^3r e^{-i\kappa \cdot \mathbf{r}} |w(\mathbf{r})|^2 \right|^2. \quad (34)$$

A completely filled lattice, i.e.,  $N \geq N_L$ , with a large number of lattice sites will have a correspondingly large number of atoms, so that the superfluid ground state is well-described by a coherent state with an average of  $N$  atoms. Then we have as before that  $\langle \hat{n}_j \hat{n}_k \rangle = \bar{n}^2$  ( $j \neq k$ ) and  $\langle \hat{n}_j^2 \rangle = \sigma^2 + \bar{n}^2$ . The expression for the cross section, valid in both the superfluid and Mott insulating phases, is given by,

$$\frac{1}{a_s^2} \frac{d\sigma}{d\Omega} = \left( \bar{n}^2 \left| \sum_{j=1}^{N_L} e^{-i\kappa \cdot \mathbf{R}_j} \right|^2 + \sigma^2 N_L \right) \left| \int d^3r e^{-i\kappa \cdot \mathbf{r}} |w(\mathbf{r})|^2 \right|^2. \quad (35)$$

In this expression, the first term gives elastic Bragg peaks that scale as the square of the number of atoms in the lattice. The remaining term gives the inelastic cross section, which contributes a smooth background. In the high probe energy regime, the inelastic background is directly proportional to the fluctuations. Its amplitude will therefore be reduced as the interaction strength between the atoms in the lattice is increased relative to the tunneling matrix element. The fluctuations are shown as a function of the parameter  $U/J$  in Fig. 3 for a lattice with  $N = 6$  atoms and  $N_L = 6$  lattice sites. This is sufficient due to the rapid convergence of the shape of the decay of the fluctuations with increasing lattice size [24]. The sum over exponentials in the first term yields Bragg peaks located at positions for which  $\kappa$  is a reciprocal lattice vector. These arise due to the coherent overlap of the scattered waves from individual atoms in the lattice. Our result for the cross section recreates the expected behavior, in which, deep in the Mott insulator phase, with  $\sigma^2 \rightarrow 0$ , no inelastic background remains, whereas the superfluid phase, in which  $\sigma^2 \approx \bar{n}$ , yields an inelastic background proportional to the number of atoms in the lattice,  $N$  (see Fig. 4).

The final factor, which is the Fourier transform of the Wannier function, leads to an overall envelope with an approximately Gaussian shape. In the region between the extremes of very weakly or very strongly interacting atoms in the lattice, the fluctuations can be directly observed by measuring the scale of the inelastic background. In particular, the difference between the cross section for an arbitrary value of  $U/J$  and the cross section deep in the Mott insulator regime will eliminate the elastic Bragg peaks, and leave only a Gaussian background that scales as  $\sigma^2 N_L$ . This result is intuitively satisfying in that we can trace the impact of the density fluctuations to the incoherent part of the scattering. This is made explicit through our analysis of the interferometer, and likewise is consistent with our expectations for the scattering cross section, in which we associate the inelastic part of the cross section with incoherent scattering processes.

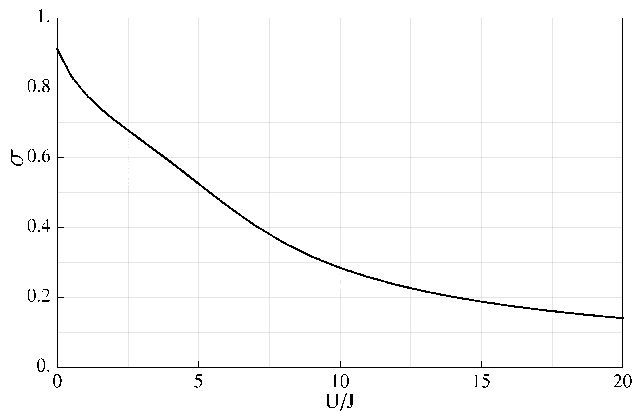


FIG. 3. The on-site number fluctuations,  $\sigma$ , plotted as a function of the parameter  $U/J$ , for a lattice with  $N = 6$  atoms and  $N_L = 6$  lattice sites and a depth of  $s = 15$  times the photon recoil energy.

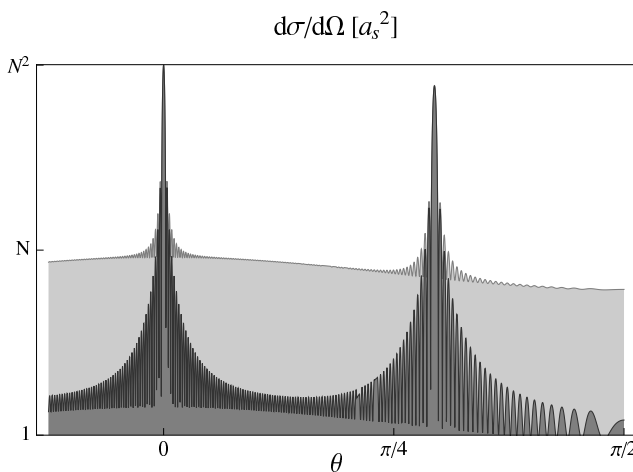


FIG. 4. The cross section given by Eq. (35) for scattering a matter wave from the atoms in a one-dimensional lattice, oriented perpendicular to the incident probe wave vector, as a function of the angle  $\theta$  from the forward direction. The first term in the cross section, which gives Bragg peaks, are computed for 100 atoms in 100 lattice sites. The second term, giving the inelastic background, is plotted using the values of  $\sigma$  given in Fig. 3 and a tunneling matrix element  $J = 0.0047 E_r$ . The plot in light gray corresponds to  $U/J = 0$ , in which the target is entirely superfluid. The small deviation from  $N$  is a result of using the exact, non-interacting ground state, rather than the coherent state approximation. The cross section for scattering from a target with  $U/J = 20$  is shown in dark gray.

#### IV. CONCLUSIONS

We have shown that matter wave scattering is susceptible to the purely quantum mechanical fluctuations in on-site atom number in an optical lattice. The fluctuations lead to incoherent scattering of the probe atom, which can be quantified and observed by the loss of contrast of the interference fringes in a Mach-Zender interferometer. The fringes form due to the interference between the scattered matter wave and the unscattered, reference arm of the interferometer. To first order in the interaction strength,  $V_0$ , the interference pattern is shifted due to a quantum mechanical phase proportional to the density of atoms in the lattice. Decoherence occurs in the interferometer as a second order effect. The second order term in a Born series expansion of the many body scattering  $T$ -matrix, proportional to  $V_0^2$ , corresponds physically to double scattering of the probe within the cold atom sample. When this multiple scattering is taken into account, the scattered matter wave becomes sensitive to the local density fluctuations in the target, which cause decoherence of the probe atom.

In the regime in which the scattered probe atom has an energy that is large compared to the bandwidth of the lowest band of the optical lattice, the fluctuations can be directly obtained from the amplitude of the inelastic scattering background. Whereas the elastic part of the scattering cross section corresponds to coherent scattering, the inelastic part contains the incoherent contribution, in which atoms in the lattice are excited out of the ground state. This

incoherent process exhibits a simple and direct dependence on the density fluctuations, providing a method to directly observe them.

### ACKNOWLEDGMENTS

The authors gratefully acknowledge useful discussions with Eric Heller.

### Appendix A: Derivation of $F^{(2)}(\mathbf{k}_0)$

We will evaluate the two-point scattering function given in Eq. (27),

$$F^{(2)}(\mathbf{k}_0) = \int d^3r d^3r' e^{i\mathbf{k}_0 \cdot (\mathbf{r}' - \mathbf{r})} |w(\mathbf{r})|^2 G_0(\mathbf{r}, \mathbf{r}'; E_0) |w(\mathbf{r}')|^2, \quad (\text{A1})$$

explicitly for the case of a one-dimensional lattice, in which the atoms are tightly confined in the  $y$  and  $z$ -directions, and the wave vector  $\mathbf{k}_0$  of the incident probe atom points along the  $z$ -direction. Strictly speaking, the range of the integration is over the length of the lattice; however, the locality of the Wannier function allows us to extend the integration to all space. For a harmonic confinement that is deep in the  $y$  and  $z$ -directions, the Wannier function approaches  $|w(\mathbf{r})|^2 \approx |w(x)|^2 \delta(y) \delta(z)$ . The one-dimensional case, with the substitution  $u = x - x'$ , therefore yields,

$$F^{(2)}(\mathbf{k}_0) = -\frac{m}{2\pi\hbar^2} \int_{-\infty}^{+\infty} du \frac{e^{ik_0|u|}}{|u|} \int_{-\infty}^{+\infty} dx' |w(u+x')|^2 |w(x')|^2. \quad (\text{A2})$$

We can use the harmonic approximation for the Wannier function in a lattice of depth  $s = V_0/E_r$ ,

$$w(x) \approx \left( \frac{2m_T}{\hbar^2\pi} E_r \sqrt{s} \right)^{1/4} \exp\left( -\frac{2m_T}{\hbar^2} E_r \sqrt{s} x^2 / 2 \right). \quad (\text{A3})$$

This allows us to compute the integral over  $x'$  in Eq. (A2) analytically. The imaginary part of  $F^{(2)}(\mathbf{k}_0)$  is then given by

$$\text{Im} \left( F^{(2)}(\mathbf{k}_0) \right) = -\frac{m m_T^{1/2} (s E_r^2)^{1/4}}{2\pi^{3/2} \hbar^3} 2 \int_0^\infty du \frac{\sin(k_0 u)}{u} e^{-\frac{m_T}{\hbar^2} \sqrt{s} E_r u^2}. \quad (\text{A4})$$

Notice that we have taken advantage of the evenness of the integrand to reduce the range of the integration to  $[0, \infty)$  and thereby eliminated the need for the absolute value operation on  $u$ . The remaining integral over  $u$  is then given by

$$\text{Im} \left( F^{(2)}(\mathbf{k}_0) \right) = -\frac{m k_L}{\hbar^2 2^{3/2} \sqrt{\pi}} s^{1/4} \text{Erf} \left( \frac{k_0/k_L}{\sqrt{2} s^{1/4}} \right). \quad (\text{A5})$$

- 
- [1] M. P. A. Fisher, P. B. Weichman, G. Grinstein, and D. S. Fisher, *Phys. Rev. B*, **40**, 546 (1989).
  - [2] M. Greiner, O. Mandel, T. Esslinger, T. W. Hänsch, and I. Bloch, *Nature*, **415**, 39 (2002).
  - [3] I. Bloch, J. Dalibard, and W. Zwerger, *Rev. Mod. Phys.*, **80**, 885 (2008).
  - [4] V. I. Yukalov, *Laser Physics*, **19**, 1 (2009).
  - [5] W. S. Bakr, J. I. Gillen, A. Peng, S. Fölling, and M. Greiner, *Nature*, **462**, 74 (2009).
  - [6] I. B. Mekhov, C. Maschler, and H. Ritsch, *Phys. Rev. Lett.*, **98**, 100402 (2007).
  - [7] M. Karski, L. Förster, J. M. Choi, W. Alt, A. Widera, and D. Meschede, *Phys. Rev. Lett.*, **102**, 053001 (2009).
  - [8] K. D. Nelson, X. Li, and D. S. Weiss, *Nature Phys.*, **3**, 556 (2007).
  - [9] J. F. Sherson, C. Weitenberg, M. Endres, M. Cheneau, I. Bloch, and S. Kuhr, *Nature*, **467**, 68 (2010).
  - [10] S. N. Sanders, F. Mintert, and E. J. Heller, *Phys. Rev. Lett.*, **105**, 035301 (2010).
  - [11] K. Wódkiewicz, *Phys. Rev. A*, **43**, 68 (1991).
  - [12] P. R. Berman, ed., *Atom Interferometry* (Academic Press, 1997).
  - [13] A. D. Cronin, J. Schmiedmayer, and D. E. Pritchard, *Rev. Mod. Phys.*, **81**, 1051 (2009).
  - [14] S. M. Tan and D. F. Walls, *Phys. Rev. A*, **47**, 4663 (1993).

- [15] S. N. Sanders, F. Mintert, and E. J. Heller, *Phys. Rev. A*, **79**, 023610 (2009).
- [16] J. Schmiedmayer, M. S. Chapman, C. R. Ekstrom, T. D. Hammond, S. Wehinger, and D. E. Pritchard, *Phys. Rev. Lett.*, **74**, 1043 (1995).
- [17] M. S. Chapman, T. D. Hammond, A. Lenef, J. Schmiedmayer, R. A. Rubenstein, E. Smith, and D. E. Pritchard, *Phys. Rev. Lett.*, **75**, 3783 (1995).
- [18] M. L. Goldberger and K. M. Watson, "Collision theory," (John Wiley and Sons, Inc., 1964) Chap. 3.
- [19] M. L. Goldberger and K. M. Watson, "Collision theory," (John Wiley and Sons, Inc., 1964) Chap. 3, pp. 80–82.
- [20] J. J. Sakurai, "Modern quantum mechanics," (Addison-Wesley, 1994) p. 389.
- [21] E. Fermi, "Nuclear physics," (University of Chicago Press, 1950) pp. 201–202.
- [22] L. Van Hove, *Phys. Rev.*, **95**, 249 (1954).
- [23] R. C. Forrey, L. You, V. Kharchenko, and A. Dalgarno, *Phys. Rev. A*, **54**, 2180 (1996).
- [24] J. M. Zhang and R. X. Dong, *Eur. J. Phys.*, **31**, 591 (2010).